LWT - Food Science and Technology xxx (xxxx) 113419

Contents lists available at ScienceDirect

LWT - Food Science and Technology

journal homepage: www.elsevier.com/locate/lwt

Self-association of caseinomacropeptide in presence of $CaCl_2$ at neutral pH: Calcium binding determination

Karina G. Loria [a, b], Ana M.R. Pilosof [c], María E. Farías [a, d, *]

[a] Universidad Nacional de Luján, Departamento de Tecnología, Ruta 5 y 7, Luján, 6700, Buenos Aires, Argentina
[b] CONICET, Consejo Nacional de Investigaciones Científicas y Técnicas, Argentina
[c] ITAPROQ-CONICET, Universidad de Buenos Aires, Facultad de Ciencias Exactas y Naturales, Departamento de Industrias, Ciudad Universitaria, Buenos Aires, 1428, Argentina
[d] CIC, Comisión de Investigaciones Científicas de la, Provincia de Buenos Aires, Argentina

ARTICLE INFO

Keywords:
Calcium binding peptides
Calcium binding isotherms
Self-assembly

ABSTRACT

The caseinomacropeptide (CMP) is a bioactive peptide produced during cheese making. It is found in abundance in whey. CMP aqueous solutions allow the incorporation of large amounts of $CaCl_2$ but the mechanism of calcium-CMP interactions are unknown. In order to evaluate its calcium binding capacity, the following techniques were performed: Dynamic Light Scattering (DLS), Fourier Transform Infrared spectroscopy (FTIR), dialysis, conductivity, precipitation of $CaCl_2$/CMP complex by ethanol, electrochemical Ca^{2+} binding isotherms, and inhibition of calcium phosphate precipitation. One mole of CMP can bind 9 mol of calcium, and the CMP self-assembles as a hexameric form. A model is proposed to explain the CMP self-association in presence of $CaCl_2$.

1. Introduction

The calcium salts usually have low solubility at neutral/alkaline pH (Vavrusova & Skibsted, 2014). The peptides can bind calcium, thereby increasing calcium ion solubility and thus enhancing calcium absorption. During digestion of food, pH increases when the chyme is transferred from the stomach to the duodenum, which affects the binding of calcium to amino acids, peptides, and proteins with an increasing affinity (Jiang, Liu, de Zawadzki, & Skibsted, 2021). In the literature, numerous peptides of different origins have been proposed as calcium binders: for example, the peptides obtained from the fishbone (Chen et al., 2019), cucumber (Wang et al., 2017), soy (Bao, Song, Zhang, Chen, & Guo, 2007), egg yolk (Zhang et al., 2021) and dairy origin such as casein phosphopeptides or whey proteins (Berrocal et al., 1989; Zhao, Huang, Cai, Hong, & Wang, 2014). However, the commercial use for most of them is very limited mainly due to the difficulty of obtaining them on an industrial scale (Korhonen & Pihlanto, 2006).

On the other hand, the caseinomacropeptide (CMP) is a bioactive peptide produced during cheese making. It is found in abundance in whey. Likewise, it is commercially available purified by ion exchange resins. It has interesting functional properties such as gelation, foaming, and emulsifying capacity (Farías, Martinez, & Pilosof, 2010; Kreuβ, Strixner, & Kulozik, 2009; Loria, Aragón, Torregiani, Pilosof, & Farías, 2018; Martinez, Carrera Sánchez, Rodríguez Patino, & Pilosof, 2012). It also has valuable bioactive properties, among them, modulates immune systems responses, promotes bifidobacterial growth, suppresses gastric secretions, and regulates blood circulation (Thöma-Worringer, Sørensen, & López-Fandiño, 2006). The fact that CMP has no Phe in its amino acid composition makes it suitable for nutrition for the management of phenylketonuria (Ney, Hull, van Calcar, Liu, & Etzel, 2008). Its peptidic sequence contains two Asp, seven or eight Glu residues (depending on the variant CMP B or A, respectively), a phosphorylated Ser, and three Lys residues. Approximately 50% of the 19 CMP isoforms are glycosylated in commercial caseinomacropeptide (Sunds, Poulsen, & Larsen, 2019). The sialic acid (recognized calcium binder) is between 5 and 11 g/100 g of the total CMP (Fernando & Woonton, 2010). At pH 7.0 and in the absence of salts, all acidic AA side chains of CMP are deprotonated, the zeta potential is approximately −20 mV for non-glycosylated CMP (aCMP) and −30 mV for glycosylated CMP fraction (gCMP) so self-association is prevented due to the repulsion by the strong negative charge (Kreuβ et al., 2009) being the monomeric form predominant (Farías et al., 2010).

Abbreviations: CMP, caseinomacropeptide; DLS, dynamic light scattering; FTIR, Fourier transform infrared spectroscopy; ISE, ion selective electrode; d*(H)*, hydrodynamic diameter

* Corresponding author. Universidad Nacional de Luján, Departamento de Tecnología, Ruta 5 y 7, Luján, 6700, Buenos Aires, Argentina.
E-mail address: efarias@unlu.edu.ar (M.E. Farías).

https://doi.org/10.1016/j.lwt.2022.113419
Received 30 September 2021; Received in revised form 15 March 2022; Accepted 30 March 2022
0023-6438/

Considering its functional and bioactive properties, it is important to investigate the calcium binding capacity of CMP to develop calcium supplements. A relevant antecedent of this study was carried out by Burns et al. (2015): the growing mice had enhanced femoral calcium contents receiving low calcium and a CMP supplemented diet. These results highlight the potential of CMP on bone health. CMP aqueous solutions can be an excellent alternative to increase calcium bioavailability in foods because to allow the incorporation of large amounts of $CaCl_2$, but its binding capacity and mechanism are unknown (Loria, Pilosof, & Farías, 2018).

The purpose of this study was to evaluate the calcium binding capacity of CMP at neutral pH and to reveal its calcium binding mechanism by a series of techniques.

2. Materials and methods

2.1. Samples preparations

BioPURE-GMP® (CMP) was supplied by AGROPUR (Le Sueur, MN, USA). Its composition was: 863 g/kg protein, nitrogen to a protein conversion factor of 7.07. The quantity of NeuNAc was specified between 7 and 8 g/100 g (Fernando & Woonton, 2010). The calcium content of the CMP powder determined with an atomic absorption spectrometer was 6.80 g/kg using the AAnalyst 200 PerkinElmer analyzer (PerkinElmer, Shelton, CT, USA). The average CMP molecular weight was considered 7.5 kDa. Analytical grade calcium chloride anhydrous ($CaCl_2$) was supplied by Merck (Darmstadt, Germany).

The CMP solutions were obtained by dissolving the appropriate quantity of CMP powder in ultrapure water (1.8 ± 0.1 mS/cm) and stirring at room temperature for 1 h. Briefly, CMP solution was added into $CaCl_2$ solution at the final $CaCl_2$/CMP molar ratios ranging from 1 to 30. CMP is highly soluble in water and no precipitate was formed after adding $CaCl_2$. The pH of the aqueous solutions was adjusted to 7.0, 8.0, or 9.0 by the addition of a few drops of 1 mol/L NaOH to avoid dilution. The glass materials were washed with 0.01 mol/L ethylenediamine tetra-acetic acid (EDTA), 2 g/100 g $HNaCO_3$, and 0.1 g/100 sodium dodecylsulphate to remove trace element impurities (Roig, Alegría, Barberá, Farré, & Lagarda, 1999) and then rinsed three times in ultrapure water.

2.2. Atomic absorption spectrometry

Determinations of calcium were carried out by atomic absorption spectrometry using the AAnalyst 200 PerkinElmer analyzer (PerkinElmer, Shelton, CT, USA). Lanthanum nitrate (15 g/L) was previously added to standards, samples, and controls to avoid phosphate interference.

2.3. Particle size measurement

The particle size of the samples was tested by dynamic light scattering (DLS) (Zetasizer Nano-Zs, Malvern Instruments, Malvern, UK) at a fixed scattering angle of 173° as reported previously in Loria, Pilosof, and Farías (2018). The intensity particle size distribution can be converted, using the Mie theory, to volume size distribution as was described in (Martinez, Carrera Sánchez, Patino, & Pilosof, 2009). The concentrations of the CMP solutions were 30 and 50 g/L, the $CaCl_2$/CMP molar ratios ranged from 0 to 30; pH 7; 25 °C. The assay was performed in triplicate on three individual samples.

2.4. Fourier transform infrared spectroscopy (FTIR)

The samples at pH 7.0 (CMP concentration: 150 g/L; $CaCl_2$/CMP molar ratios: 0, 2, 9 and 15) were stored in a freezer at a temperature of −80 °C for 24 h and subsequently lyophilized (Labconco Freezone 12 L Freeze dry System Model 77540, Labconco, Kansas City, MO, USA) for 48 h until a dry sample was obtained. The mixtures of 1 mg of each lyophilized sample and 100 mg dry KBr were loaded on the FTIR instrument (Shimadzu®, IRPrestige-21, Tokyo, Japan). The spectra were obtained using 40 scans from 4000–500 cm^{-1} at a resolution of 2 cm^{-1}. The peak signals were analyzed with the OriginPro ®8 SR0 software V8.0724 (OriginLab Corporation, Northampton, MA, USA).

2.5. Calcium binding capacity by dialysis

The solution sample (CMP concentration: 10 g/L; $CaCl_2$/CMP molar ratio:15, pH 7.0) was maintained 30 min at room temperature. A volume of 5 mL of the solution was transferred to a dialysis bag (Ester Cellulose from Biotech, MWCO: 100–500 Da, Spectrum Laboratories Products, Inc., Rancho Dominguez, CA, USA). Due to the important influence of the ionic strength of CMP self-association, the samples were dialyzed under stirring against 250 mL of ultrapure water (pH 7.0) for 24 h to remove the free Ca^{2+} at 25 °C. The dialysate was changed every 8 h. Calcium concentration was determined by atomic absorption spectroscopy. Control of CMP (10 g/L) was simultaneously dialyzed. The assays were performed in triplicate.

Dialysis percentages were calculated as follows (**equation (1)**):

$$\text{Dialysis percentage} = 100 \times D/C, \quad (1)$$

where D is the calcium content of the dialysis bag, and C the total calcium content of the sample.

2.6. Calcium binding determination by conductivity measurement

The calcium binding capacity of CMP was carried out according to the method described in Valente et al. (2011) with slight modifications. The electric conductivity of the 7.5 mL of $CaCl_2$/CMP solutions (0–15 M ratio) was measured by a conductivity meter model HI2003-02 with a digital 4 ring conductivity probe with integrated temperature sensor HI 763100 (Hanna Instruments, Nusfalau, Romania) at 25 °C. The equipment was calibrated with standard solutions: 1413 μS/cm (Hanna Instruments, HI 70031); 5000 μS/cm (Hanna Instruments, HI 70039) and 12,880 μS/cm (Hanna Instruments, HI 70030). The tests were carried out for quadruplicate. The variation of the molar conductivities ($\Delta\kappa$, expressed as S cm^2/mol) of $CaCl_2$ in the presence, κ_{CMP}, and the absence, κ, of CMP was calculated using **equation (2)**:

$$\Delta\kappa = \left(\kappa_{CMP} - \kappa\right)/c\ CaCl_2 \quad (2)$$

c $CaCl_2$ is the $CaCl_2$ molar concentration.

2.7. Calcium/CMP complex precipitated by ethanol

The calcium/CMP samples were prepared in a 50 mL flask, by adding 1 mL of 0.04 mol/L $CaCl_2$ at 4 mL of 1.0, 1.5, 2.0, or 2.5 g/L CMP solution according to the method described in Zhao et al. (2014) with slight modifications. After 30 min of stirring at 25.0 °C, absolute ethanol (45 mL) was added to the solution to remove the unbound calcium ions. The pH of the solution was adjusted to 7.0 by the addition of 0.1 mol/L NaOH. After centrifugation (10,000 g at 4 °C for 10 min), the content of calcium in the supernatant (unbound calcium) was measured by EDTA complexometric titration method (Zhao, Vavrusova, & Skibsted, 2018). The amount of calcium bound to CMP, Ca_B, (expressed as a molar ratio) was determined by the difference between the calcium total concentration, Ca_T, and the determined calcium concentration by titration in the supernatant, Ca_S, divided the molar concentration of CMP, c (**equation (3)**):

$$Ca_B = (Ca_T - Ca_S)/c \quad (3)$$

Total calcium concentrations were assayed by atomic absorption spectrophotometer. The determination assumes that CMP was totally precipitated by absolute ethanol. The assay was performed in triplicate on three individual samples.

2.8. Calcium binding constants

Calcium-binding was investigated using the method of Berrocal et al. (1989) with modifications. Calcium ion activity was measured with an ion selective electrode (ISE) (model HI4104), connected to a Hanna Instruments Waterproof Portable (model HI98191, Hanna Instruments, Nusfalau, Romania) after each 50 μL $CaCl_2$ addition (0.2 mol/L) on 50 mL 2.0 g/L CMP solution under constant stirring. The maximum added volume of $CaCl_2$ was 2 mL. Ionic strength was adjusted to 0.1 mol/L with KC1. The pH was kept constant at the desirable value (7.0, 8.0, and 9.0) by addition 0.1 mol/L NaOH at 25 °C. The tests were carried out in triplicate. The electrode was calibrated with standard calcium solutions.

The free calcium concentration in the samples, (Ca_F), was estimated assuming unity activity coefficients. The bound Ca (Ca_B) was calculated by subtracting Ca_F concentration from the total calcium concentration (Ca_T) (**equation (4)**). The total calcium concentrations were determined by atomic absorption spectroscopy as detailed Section 2.2:

$$Ca_B = Ca_T - Ca_F \quad (4)$$

The apparent association constants (K_{app}) and the maximum bound Ca per mol of CMP (n_i) were calculated using a Klotz plot analysis (Zhang, Geng, Huang, & Ma, 2016). The values of the inverse of Ca_B were plotted as a function of the inverse of Ca_F according to **equation (5)**:

$$\frac{1}{Ca_B} = \frac{1}{n_i\ K_{app}\ Ca_F} + \frac{1}{n_i} \quad (5)$$

K_{app} was defined by Vavrusova and Skibsted (2014) (**equation (6)**), being $[L]^-$ the ligand (CMP):

$$K_{app} = \frac{[CaL]^+}{[L]^-[Ca]^{2+}} \quad (6)$$

2.9. Inhibition of calcium phosphate precipitation

The calcium phosphate precipitation was performed according to Jung et al. (2006) with some modifications. The CMP solutions (0.3–5.0 g/L final concentration) were prepared in a 100 mL flask, then adding a fixed volume of $CaCl_2$ solution (5.0 mmol/L final concentration) and finally 30 mL of 0.02 mol/L sodium phosphate buffer (pH 7.8). The solutions were stirred at 25 °C for 1 h. Next, it was centrifuged at 3000 g for 20 min. The supernatant (calcium/CMP samples) obtained was filtered with a 0.45 μm Millipore® membrane filter. The content of calcium in the supernatant was determined by atomic absorption spectrometry (Section 2.2).

The amounts of calcium bound to CMP, CaB, (expressed as a molar ratio) were divided by the content of calcium in the supernatant (mol/L), CaS, by the molar concentration of CMP, c, according to **equation (7)**.

$$CaB = CaS\ /c \quad (7)$$

The experiment was performed in triplicate, and the calcium binding capacity was expressed as mean ± standard error. The ultrapure water was used as a control.

2.10. Data analysis

Graphs and statistics were generated using Prism v8.0.1 (GraphPad Software, San Diego, CA, USA) where results are presented as mean ± standard deviation (SD) unless otherwise stated. Statistical analysis was performed using one-way ANOVA with either a Tukey's (parametric) or Kruskal-Wallis (non-parametric).

3. Results and discussion

3.1. Particle size

DLS measurements of $CaCl_2$/CMP solutions were performed to evaluate the impact of $CaCl_2$ presence at the molecular level. Without interaction between CMP and calcium, it would be expected that the characteristic particle sizes for CMP would be maintained and, conversely, an increase in size would be indicative of molecular interaction. All solutions showed multimodal intensity size distributions (data not shown), but from volume size distributions it was possible to deduce the relative proportion of the populations. The first peak population accounted the 29.9 percent of the particle by intensity that represented the 99.9 percent of the particle by volume. So, the populations with higher size (40–300 nm) were negligible and only the lower size peak was the predominant (Farías et al., 2010). The intensity size distribution of salt free CMP solutions at pH 7.0 and 25 °C presented three populations. The hydrodynamic diameter, d*(H)*, of the predominant size peak ranged between 1 and 5 nm. The maximum value of the predominant size peak was 2.3 nm, corresponding to the CMP monomer according to Zetasizer Nano-Zs equipment software as it was previously reported by Farías et al. (2010). According to Kreuβ et al. (2009), the hydrophobic domains of CMP (AA 1–5, 17–22, 35–39 and 58–65) are more or less shielded by the negative charge density of the Glu and Asp residues. This effect is more pronounced for gCMP due to the negative charge of the terminal sialic acid residues. While the C-terminus and a huge part of the peptide have a strong negative charge, there are three small positively charged domains at the N-terminus. So, the individual CMP molecules show a tendency to keep each other at distance.

When calcium chloride was added, the d*(H)* of the predominant first peak shifted to higher sizes, from 2.3 nm (salt free solution) to 5.6 nm ($CaCl_2$/CMP molar ratio 9) indicating a molecular association as was described in Loria, Pilosof, and Farías (2018). From the *d*(H) corresponding to the maximum values of the predominant size peaks in the intensity size distributions, it could be estimated the molecular weight (MW) of the peptide by a tool in the Zetasizer Nano-Zs software. From the MW, the predominant association state of CMP at each $CaCl_2$/CMP molar ratio at pH 7.0 can be calculated as a relation between the MW corresponding to the diameter of the maximum value of the lower size peak and the MW of the CMP monomer. The d*(H)* of the predominant size peak and association state of two CMP concentrations (10 and 50 g/L) is plotted as a function of the $CaCl_2$/CMP molar ratio in Fig. 1. The predominant size peak moved towards higher values to 3.6 nm (dimeric form), 4.8 nm (tetrameric form), and finally reached a maximum value to 5.6 nm (hexameric form) for $CaCl_2$ addition, indicating molecular self-association. The monomeric form was not present once CMP was self-associated as dimers, tetramers, or hexamers. Regardless of peptide concentration (10 or 50 g/L), the maximum state of association (5.6 nm) was obtained for $CaCl_2$/CMP molar ratios between 7.5 and 9. With increased ionic strength, the net surface charge of the molecules is decreased and therefore the repulsive forces between single molecules decrease as well (Kreuβ et al., 2009). As it was previously reported in Loria, Pilosof, and Farías (2018), CMP self-assembled in presence of NaCl. However, the maximum state of association was the tetrameric form. On the other hand, the turbidity of $CaCl_2$/CMP solutions increases over storage, while the NaCl/CMP solutions are stable (Loria, Pilosof, & Farías, 2018). This result is a clear indication that the

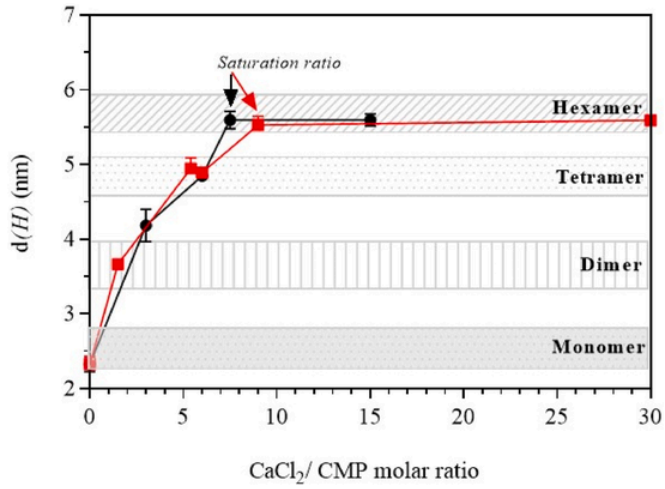

Fig. 1. Hydrodynamic diameter, d*(H)*, of the predominant lower size peak from particle size distributions at pH 7.0 and 25 °C for solutions of caseinomacropeptide at 10 g L^{-1} (●) and 50 g L^{-1} (■) as a function of $CaCl_2$/CMP molar ratios (0–30 mol/mol). Data are given as mean ± standard error, n = 3.

nature of the cation has an important influence on the CMP self-assembly.

3.2. Fourier transform infrared spectroscopy

The infrared spectroscopy technique is used to verify whether a mineral-peptide interaction occurred (Luo, Yao, Soladoye, Zhang, & Fu, 2022). The FTIR spectrum of free salt CMP from 4000–500 cm^{-1} wavenumber was shown in Fig. 2 (please see molar ratio 0). This spectrum is similar to that extensively described by Burgardt et al. (2014). As can be seen, a wide and intense band near 3300 cm^{-1} related to an overlap of bands corresponding to the O–H stretching vibration, free or H bonded (Burgardt et al., 2014). The secondary amide A and B bands related to proline residues, abundant in CMP, are found at 3300 cm^{-1} and 3080 cm^{-1}, respectively (Burgardt et al., 2014). The two most prominent vibrational bands of the proteins/peptides are the Amide I vibration (1700 to 1600 cm^{-1}), which is mainly caused by stretching of

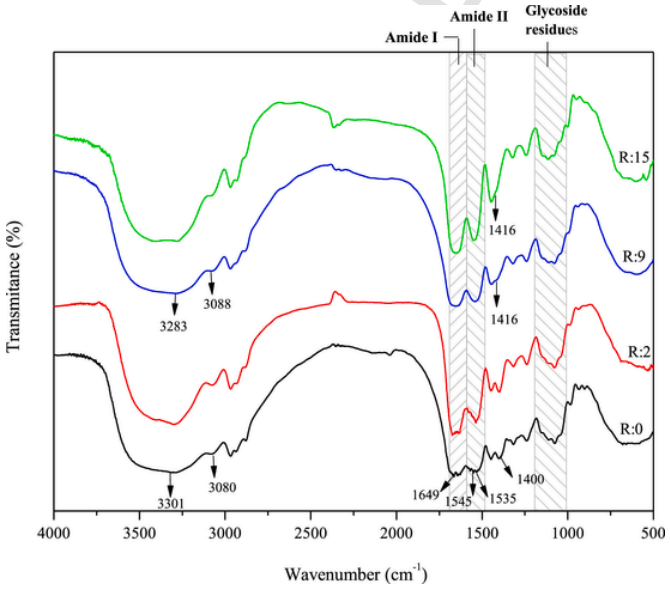

Fig. 2. FTIR spectrum of $CaCl_2$/CMP at different molar ratios, R: (–) 0; (–) 2; (–) 9 and (–) 15 over a wavenumber region between 4000 cm^{-1} to 500 cm^{-1} at a resolution of 2 cm^{-1} and pH 7.0.

C═O bonds, Amide II vibration (1600 to 1500 cm^{-1}), which is produced by the deformation of NH bonds and stretching of CN bonds (Zhao et al., 2014). These bands in CMP spectra were observed at 1649 cm^{-1} (Amide I) and 1545 and 1535 cm^{-1} (Amide II). The strong absorbance band at 1400 cm^{-1} in the CMP spectrum at pH 7 indicates that the carboxylate functional group (COO^-) is present because Asp and Glu residues are deprotonated. The glycoside residue signal in the fingerprint region is attributed between 1200 and 1000 cm^{-1} (Khajehpour, Dashnau, & Vanderkooi, 2006). According to Lewis, Lewis, and Lewis (2013), sialic acid has a characteristic signal at 1024 cm^{-1}, N-Acetylglucosamine (GlcNAc) at 1025 cm^{-1}, and N-Acetylgalactosamine (GalNAc) at 1038 cm^{-1}.

According to the absorption peak shifts in FTIR, the binding sites of calcium ions on the CMP peptide chain could be observed. As can be seen from Fig. 2, FTIR spectra of samples showed important differences between CMP and $CaCl_2$/CMP molar ratios ≥9, which indicated that some groups of amino acids had reacted after binding reaction between the CMP and calcium. The absorption at a high frequency of 3301 cm^{-1} (Amide 2° A) which is attributed to the vibration of N–H stretching moved to 3283 cm^{-1} and that of Amide 2° B from 3080 to 3088 cm^{-1}, demonstrating that the N–H groups had replaced by N–Ca bonds as described by Peng, Hou, Zhang, and Li (2017) and Wang et al. (2017) for other peptides. The Amide I and II vibrations are affected by the nature of the side chain upon the interactions $CaCl_2$/CMP, and they could be related with the C–O groups that would participate in the interaction of the peptide with Ca^{2+} (Wu et al., 2019). In the Amide II region, the peaks corresponding to wavenumbers 1535 and 1545 cm^{-1} have disappeared, finding a large valley on $CaCl_2$/CMP molar ratios 9 and 15. The absorption peak of CMP generated at 1400 cm^{-1}, corresponding to the symmetric stretches of the carboxylic groups (COO^-), shifted to 1416 cm^{-1} for $CaCl_2$/CMP molar ratio ≥9 spectra. This effect can be attributed to the extension of the -COO^- groups that combine with Ca^{2+} to form COO–Ca. Similar changes in the FTIR spectra were found in calcium binding peptides from bone collagen (Luo et al., 2022); *Auxis thazard* protein hydrolysate (Chen et al., 2019); collagen peptide extracted from *Gadus macrocephalus* bone (Peng et al., 2017) and cucumber seed peptide produced by liquid state fermentation with *B. subtilis* (Wang et al., 2017).

3.3. Calcium binding capacity by equilibrium dialysis

During the first 8 h of the trial, the calcium concentration inside the dialysis bag decreased rapidly, until reaching equilibrium (24 h). The rapid decrease in the calcium fraction is due to the easy diffusion of the ions through the semipermeable membrane, which cannot be crossed by the CMP molecules. Calcium ions diffused due to the difference in chemical potential between the solution inside the bag and the water outside. Given the impact of ionic strength on the state of association of CMP, it was decided to dialyze the sample against ultrapure water at pH 7 and not against a Tris-HCl buffer solution as mentioned in the literature (Bao et al., 2007). The obtained dialysis percentage was 64.4 ± 3.3%. Considering the initial concentration of CMP, it can be estimated a $CaCl_2$/CMP molar ratio between 9 and 10. Interestingly, the dialysis percentage of the control CMP solution was 63.5 ± 1.3%. This reveals that the original CMP sample provided 0.73 ± 0.13 mol of calcium bound to CMP.

3.4. Conductivity

The conductivity of a solution is directly related to the ease of an electric current to flow through it. The more ions are free in a solution, the higher the conductivity is. The electrical conductivity of the complex solutions can be used to indirectly measure the maximum binding capacity of Ca^{2+} to the peptide (Guo et al., 2020). Electrical conductivity is dependent on particle charge changes and the size and shape of

moving particles (Valente et al., 2011). As can be seen from Fig. 3, the variation of the specific conductance of $CaCl_2$, $\Delta\kappa$ (Equation (2)), in the presence, κ_{CMP}, and absence, κ, of CMP as a function of the $CaCl_2$/CMP molar ratio. Maintaining the CMP concentration constant (20 g/L) and upon increasing salt concentration, the $\Delta\kappa$ decreases because an interaction occurs between $CaCl_2$ and the CMP, in such a way that $\Delta\kappa$ approaches zero at concentration ratios higher than the stoichiometric ratio. This value was determined at 11 $CaCl_2$/CMP molar ratio. Also, the pH slightly decreases from 6.7 to 6.0 as was reported in Loria, Pilosof, and Farías (2018). This effect is attributed to the liberation of protons due to the Ca^{2+} binding to CMP.

3.5. Calcium/CMP complex precipitated by ethanol

The peptides can be separated into different fractions through ethanol precipitation, which changes the degree of ionisation of peptides due to the different dielectric constants of ethanol (24.5) and water (78.5) (Kong et al., 2021). The ethanol precipitation is a better method to enrich low-molecular-weight metal-peptide fragments (Kong et al., 2021). The addition of alcohols to aqueous solutions decreases the polarity of protein, and favours the hydrogen bonds and α-helical structures, whereas hydrophobic interactions become less pronounced (Gülseren, Fang, & Corredig, 2012). The obtained precipitates were generally assumed to be metal chelating peptides (Kong et al., 2021; Xu et al., 2021; Zhao et al., 2014; Zong, Peng, Zhang, Lin, & Feng, 2012). This methodology allowed estimating in a semi-quantitative approach the calcium/CMP molar ratio that precipitated with the peptide. The CMP concentrations were selected until a precipitate was found. The used $CaCl_2$/CMP relation ranged from 30 to 75 M ratio. As shown in Table 1, the amount of calcium bound per mole CMP was independent of the CMP concentration in the trial, being 11 ± 2 M ratio according to the values obtained from particle size measurements (7.5–10 M ratio).

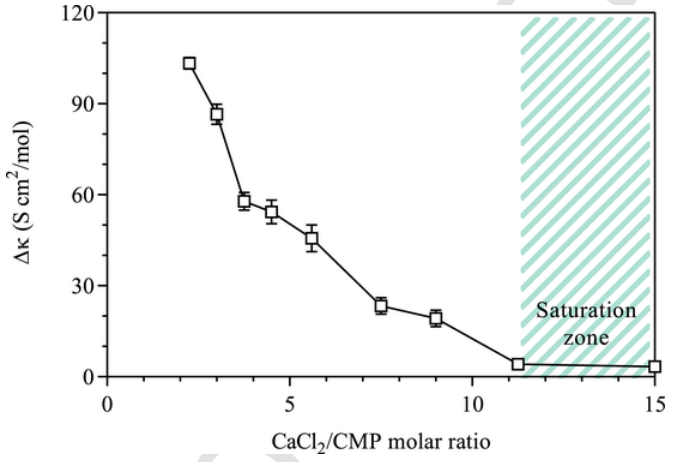

Fig. 3. Variation of the specific conductance, $\Delta\kappa = (\kappa_{CMP} - \kappa)/c$, of $CaCl_2$ solutions in the presence (κ_{CMP}) and absence (κ) of caseinomacropeptide as a function of $CaCl_2$/CMP molar ratios at 25 °C. Data are given as mean ± standard error, n = 4.

Table 1
The calcium/caseinomacropeptide (Ca^{2+}/CMP) molar ratio (Ca^{2+}/CMP) obtained by ethanol precipitation at pH 7.0 and 25 °C.

CMP concentration (g/L)	Ca^{2+}/CMP molar ratio
1.0	9 ± 2[a]
1.5	11 ± 1[a]
2.0	13 ± 1[a]
2.5	12 ± 2[a]

Data are given as mean ± sd (n = 3). Letters different represents significant differences (P < 0.5).

3.6. Calcium-binding constants of CMP

The binding isotherms (Fig. 4) indicate the presence of two types of Ca^{2+} binding sites with different affinities for the ion at pH 7.0, 8.0, and 9.0. The sites with the higher affinity are saturable, whereas the low affinity sites remain unsaturated. For the high calcium affinity zone, Ca_B remained under 10^{-4} mol/g CMP even increasing Ca_F in solution. Meanwhile, for low affinity sites, Ca_B was directly proportional to the concentration of Ca_F, without reaching a maximum value or "plateau".

The Klotz plots ($1/Ca_B$ vs $1/Ca_F$) calculated for the three pH values are shown in Fig. 5. The Klotz graphs showed two (Fig. 5 C) or three lines (Fig. 5 A and **B**) with a good fit ($R^2 > 0.911$). As well, Zhang et al. (2016) recognized two lines in the Klotz plots. They demonstrated the

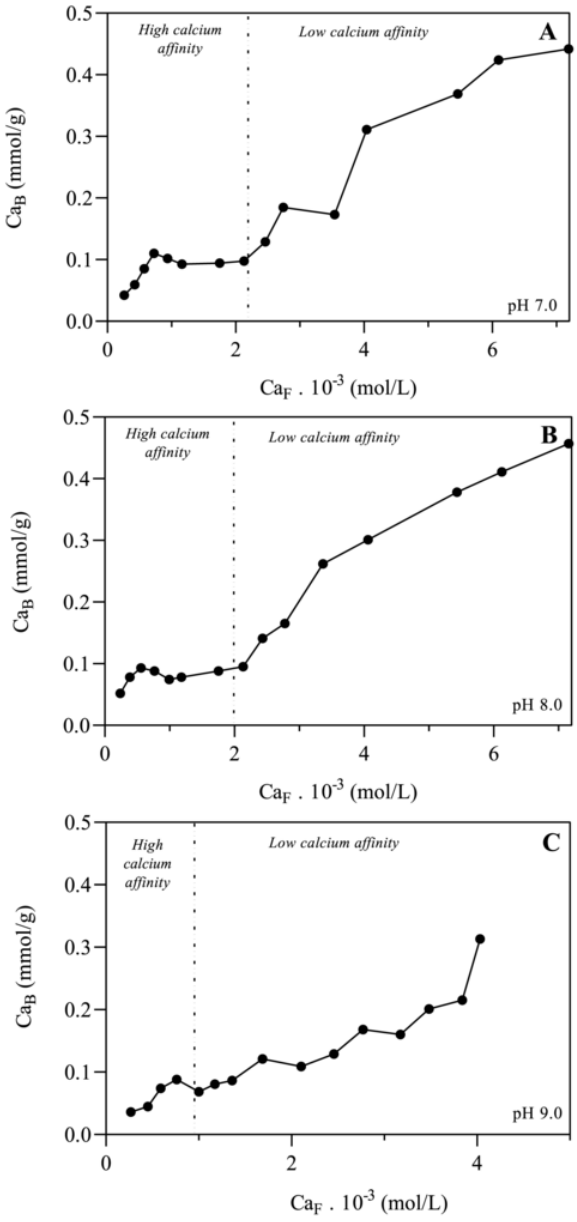

Fig. 4. Binding isotherms of caseinomacropeptide and $CaCl_2$ under different pH conditions: (**A**) pH 7.0, (**B**) pH 8.0 and (**C**) pH 9.0 at 25 °C. Data are given as mean.

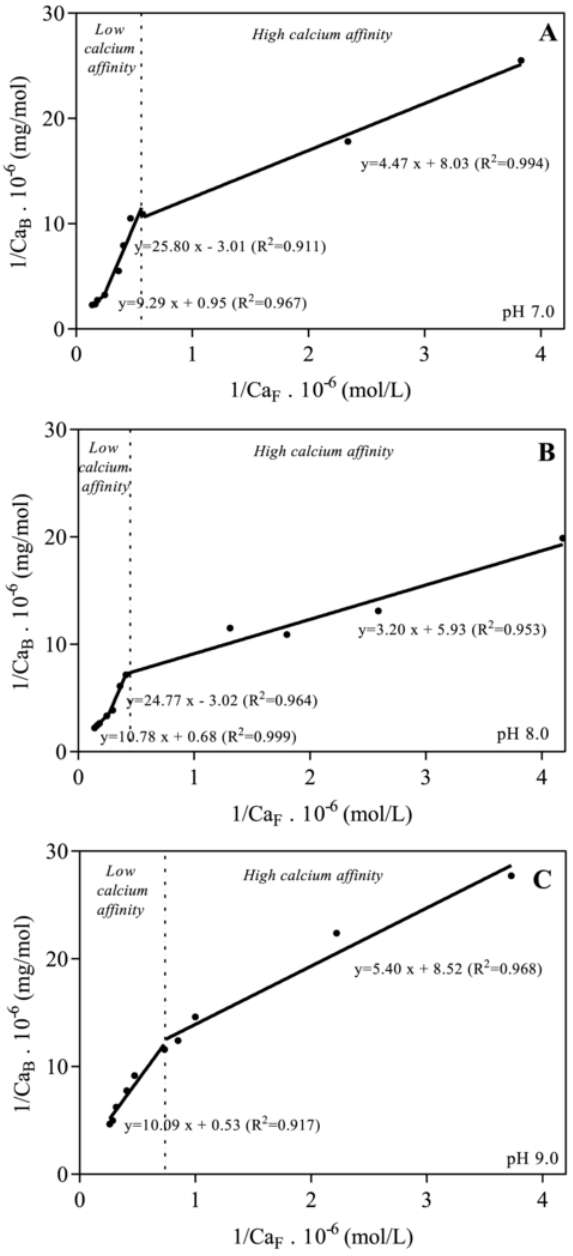

Fig. 5. Klotz plots of caseinomacropeptide and $CaCl_2$ under different pH conditions: (A) pH 7.0, (B) pH 8.0 and (C) pH 9.0 at 25 °C. Data are given as mean.

presence of two classes of calcium binding sites, that is, low and high affinity, on phosvitin. The intrinsic association constants and the number of binding sites were calculated from the intercepts and slopes of the plot, respectively. The results are shown in Table 2. For the high affinity binding sites, the association constant, K_{app}, was 2200 ± 300 L/mol independent of the pH value. The n_i was approximately 1 mol calcium bound per mole CMP. Zhang et al. (2016) found an association constant for phosvitin of approximately 10^4 L/mol for high affinity binding sites regardless of pH from 7 to 8.5, with approximately 30 mol calcium bound per mole phosvitin. Berrocal et al. (1989) mentioned that the amount of calcium bound to the peptides is directly related to their phosphorus content. The high affinity binding site is highly protonated at all three pH values, so it can be hypothesised that it is possibly a phosphorylated residue. According to Brody (2000), the

Table 2
Binding constants ***(Kapp)*** and the maximum bound Ca (n_i) obtained from Klotz plot analysis at pH 7.0; 8.0 and 9.0 for "high" and "low" affinity sites of caseinomacropeptide (CMP).

pH	High affinity sites		Low affinity sites	
	K_{app} (L/mol)	n_i (Ca^{2+}/CMP molar ratio)	K_{app} (L/mol)	n_i (Ca^{2+}/CMP molar ratio)
7.0	1700 ± 300[a]	0.93 ± 0.04[a]	132 ± 30[a]	8 ± 2[a]
8.0	2200 ± 300[a]	1.26 ± 0.21[a]	63 ± 1[a, b]	11 ± 1[a]
9.0	1600 ± 50[a]	0.9 ± 0.1[a]	33 ± 1[b]	14 ± 1[a]

Data are given as mean ± sd (n = 3). Different letters represent significant differences at P < 0.05.

Ser residue at position 44 is always phosphorylated in the CMP molecule.

In contrast, 6 to 15 calcium ions were accumulated in the low affinity binding sites of the CMP **(Table 2).** The fact that pH decreased in CMP solutions with the addition of the calcium salt. Loria, Pilosof, and Farías (2018) suggested that the low affinity binding to sites involved H^+ exchange. Among the amino acids, aspartic and glutamic are strong calcium binders. Although they are weak compared to other anions, the polypeptides have a synergistic effect (Vavrusova & Skibsted, 2014). The CMP molecule has eight Glu residues (positions 13, 24, 32, 35, 42, 46, 49, and 53), the C-terminal carboxyl group and two Asp residues at positions 10 and 43 (Brody, 2000). All of them can constitute part of calcium binding sites. Also, the CMP peptide chain has attached sialic acid residues, which are known to bind calcium. K_{app} of sialic acid is 121 L/mol, only Ca^{2+}/sialic acid molar ratio 1 is formed (Jaques, Brown, Barrett, Brey, & Weltner, 1977). Dang, Shin, Bell, Nagaswami, and Weisel (1989) measured the binding of calcium to asialo fibrinogen and untreated fibrinogen by using a calcium ion-sensitive electrode. They suggested that sialic acid residues are required for low affinity calcium binding. Considering that sialic acid (Mw 309 g/mol) is present between 5 and 11 g/100 g in CMP (Fernando & Woonton, 2010), it can be estimated that 1 mol of CMP contains between 1 and 3 mol of sialic acid. Apparently, the number of low affinity binding sites was similar to the maximum number of anionic groups in CMP. However, all charged groups of CMP are not equally available, especially because CMP molecules associate in presence of calcium ions (Fig. 1). K_{app} of high affinity binding sites values were 15–70 times higher than for the low affinity binding sites (Table 2). (Zhang et al., 2016) found K_{app} of high affinity sites 5–20 times higher than for the low affinity binding sites for phosvitin. On the other hand, the value of K_{app} decreased with an increase of pH from 7.0 to 9.0: 132 ± 30 L/mol (pH 7.0) to 33 ± 1 L/mol (pH 9) (Table 2). This could be explained in terms of the solvatation of molecules by pH increasing (Loria, Aragón, Torregiani, Pilosof, & Farías, 2018). Therefore, calcium ions were more likely to bind to the amino and carboxyl groups of peptides under the neutral environment (Luo et al., 2022). The order of magnitude of K_{app} for the low affinity binding sites was consistent with the range of binding constants reported by other researchers. (Mekmene & Gaucheron, 2011) found a K_{app} of 191 L/mol for caseinophosphopeptides (pH 6.5) and 154 L/mol for potassium caseinate (pH 6.8). Recio, Guerra, Torrado, and Skibsted (2019) studied the ability of casein hydrolysate rich in caseinophosphopeptides to form calcium complexes and determined an association constant of 125 L/mol. The calcium binding capacities of CMP (molar ratio) ranged between 7 and 11, 11–13, and 14–16 at pH 7.0, 8.0 and 9.0, respectively, contemplating all maximum number of moles of calcium that can bind 1 mol of CMP on high and low affinity sites (Table 2).

3.7. Inhibition of calcium phosphate precipitation

When $CaCl_2$ and NaH_2PO_4 exist in the system, $Ca_3(PO_4)_2$ spontaneously precipitate. The inhibition of $Ca_3(PO_4)_2$ precipitation is an indi-

Table 3
Calcium solubility in phosphate buffer (pH 7.8) as a function caseinomacropeptide (CMP) concentration.

CMP concentration (g/L)	calcium solubility (mg/L)
0	3.2 ± 0.8[a]
0.3	3.4 ± 0.3[a]
0.6	4.0 ± 0.1[a]
1.0	12.4 ± 0.5[b]
1.2	27 ± 4[c]
5.0	135 ± 2[d]

Data are given as mean ± sd (n = 3). Letters different represents significant differences (P < 0.5).

rect measure of the influence of CMP as a calcium binder. The generation of $Ca_3(PO_4)_2$ gradually produces H^+, reducing the pH value of the solution (Zhang et al., 2021). The constant pH can be maintained at 7.8 by adding NaOH solution, because low pH could increase the solubility of insoluble calcium salt (Jung et al., 2006). Table 3 shows the inhibition of calcium phosphate precipitation was dependent on CMP concentrations. The solubility of calcium in phosphate buffer (pH 7.8) in absence of CMP was very low (3.2 ± 0.8 mg/L). However, small amounts of the peptide (>1.0 g/L) inhibit significantly (P < 0.05) a formation of insoluble calcium phosphate. For example, the solubility was approximately multiplied by 4 (12.4 ± 0.5 mg/L) and by 40 (135 ± 2 mg/L) for 1.0 g/L and 5.0 g/L CMP concentration, respectively.

As reported by Jung et al. (2006) employing a similar methodology, the calcium solubility of a low molecular peptide (1442 Da) obtained from fishbone proteins *Theragra chalcogramma* was 128 mg/g. The calcium-binding capacity of tilapia protein hydrolysate was 65 mg/g protein (Charoenphun, Cheirsilp, Sirinupong, & Youravong, 2013). Therefore, the calcium binding capacity of CMP, was dependent on its concentration, with the maximal molar ratio (calcium/CMP) of approximately 5. This value was significantly different from those obtained using the other techniques. It is likely that the CMP can sequester amorphous calcium phosphate to form core-shell nanoparticles in accordance with (Follows et al., 2011) for other casein peptides.

3.8. Model proposed for calcium binding

Considering the particle size evolution in a molar saturation ratio, the self-association of CMP, the FTIR evidence of calcium/CMP interaction, the calcium binding determination obtained through dialysis and conductivity, the calcium/CMP molar ratio obtained through the ethanol precipitation of CMP and the calcium binding isotherms, a theoretical model for the explanation of CMP self-association in presence of $CaCl_2$ is proposed (Fig. 6). In the first stage ($CaCl_2$/CMP molar ratio ≤1), the monomeric CMP binds in a strong affinity site (possibly a phosphorylated residue) 1 mol of calcium ions at neutral pH. This fact is supported by the calcium fraction non dialyzable of salt free CMP aqueous solution, in agreement with the binding parameters of low affinity sites.

When calcium ions were added, the strong negative charge of CMP greatly decreased at neutral pH. After the $CaCl_2$/CMP molar ratio increased to 3, the presence of calcium ions promoted the second stage of self-association $CaCl_2$/CMP molar ratio ≤3: the formation of dimers. The repulsion by the negative charges started to decrease, allowing the N-terminal hydrophobic domain (AA 1–5), which is not covered by the negative charge, to interact first, followed by the hydrophobic domains located in the centre of the peptide chain (Kreuβ et al., 2009). The dimers formation takes place via strong interactions of hydrophobic domains. It is similar to lowering the pH 5.5 of the CMP solution, once formed, the dimers are stable (Farías et al., 2010). The formation of a dimeric structure (3.6 nm in size) allows the incorporation of one or two calcium molecules more by CMP molecule.

In the third stage, those dimers get attached by the inclusion of one or two other molecules of calcium ions forming a tetrameric structure (4.8 nm in size). Finally, in the fourth stage, tetramers incorporate one dimer structure next to one or two calcium molecules more to form a hexameric structure (5.6 nm in size). As more calcium was incorporated into CMP solution, the other negative groups (phosphates, carboxylates and glycosides) of the neighboring molecules replaced the Cl^- or OH^- counterions of calcium ions allowing the association of CMP. This would explain the increase in turbidity over storage.

4. Conclusions

The results allowed to know the affinity constants of CMP for calcium and speculate on the nature of binding sites. One mole of CMP binds an equivalent amount of calcium ions at pH 7, that is, a 1: 1 ratio with a K_{app} of ~2000 L/mol. Possibly, this high affinity site is related to phosphorylate Ser of CMP. At higher concentrations of calcium in solution, the low affinity sites of CMP can bind 6–10 mol of calcium more at with a K_{app} of ~130 L/mol. The low affinity sites involved in calcium binding would be the acid residues of Glu, Asp and sialic acid. Depend on the calcium concentration, the CMP self-assembles as a dimer, tetramer o hexamer. The CMP has a potential application as calcium supplement. Future studies will be done to assess if CMP can bind calcium at acidic pH.

CRediT authorship contribution statement

Karina G. Loria: Methodology, Validation, Formal analysis, Investigation, Writing – original draft. **Ana M.R. Pilosof:** Investigation, Resources, Project administration, Supervision, Funding acquisition. **María E. Farías:** Methodology, Validation, Resources, Investigation, Writing – review & editing, Supervision, Funding acquisition.

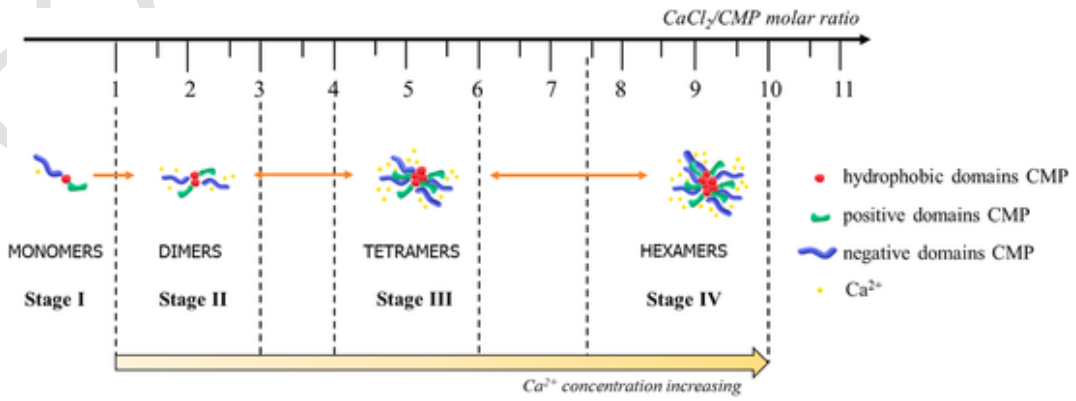

Fig. 6. Model proposed to explain the caseinomacropeptide self-association in presence of $CaCl_2$.

Acknowledgements

This research was supported by the Technology Department de of the Universidad Nacional de Luján, Agencia Nacional de Promoción Científica y Tecnológica de la República Argentina (ANPCyT) (Project: PICT-2021-CAT-I00169), Consejo Nacional de Investigaciones Científicas y Técnicas de la República Argentina (CONICET) and Comisión de Investigaciones Científicas of the Province of Buenos Aires (CIC-PBA). K.G.L. received a post-graduate fellowship from CONICET.

The authors thank Gustavo Gómez and Andrés Pighín for assisting with the mineral composition determinations.

References

Bao, X. L., Song, M., Zhang, J., Chen, Y., & Guo, S. T. (2007). *Calcium-binding ability of soy protein hydrolysates*. *Chinese Chemical Letters*, *18*(9), 1115–1118. https://doi.org/10.1016/j.cclet.2007.07.032.

Berrocal, R., Chanton, S., Juillerat, M. A., Favillare, B., Scherz, J.-C., & Jost, R. (1989). *Tryptic phosphopeptides from whole casein. II. Physicochemical properties related to the solubilization of calcium*. *Journal of Dairy Research*, *56*(3), 335–341.

Brody, E. P. (2000). *Biological activities of bovine glycomacropeptide*. *British Journal of Nutrition*, *84*(Supplement S1), 39–46. https://doi.org/10.1017/S0007114500002233.

Burgardt, V. C. F., Oliveira, D. F., Evseev, I. G., Coelho, A. R., Haminiuk, C. W. I., & Waszczynskyj, N. (2014). *Influence of concentration and pH in caseinomacropeptide and carboxymethylcellulose interaction*. *Food Hydrocolloids*, *35*, 170–180. https://doi.org/10.1016/j.foodhyd.2013.05.005.

Burns, P., Binetti, A., Torti, P., Kulozik, U., Forzani, L., Renzulli, P., et al. (2015). *Administration of caseinomacropeptide-enriched extract to mice enhances the calcium content of femur in a low-calcium diet*. *International Dairy Journal*, *44*, 15–20. https://doi.org/10.1016/j.idairyj.2014.12.005.

Charoenphun, N., Cheirsilp, B., Sirinupong, N., & Youravong, W. (2013). *Calcium-binding peptides derived from tilapia (Oreochromis niloticus) protein hydrolysate*. *European Food Research and Technology*, *236*(1), 57–63. https://doi.org/10.1007/s00217-012-1860-2. 2013.

Chen, M., Ji, H., Zhang, Z., Zeng, X., Su, W., & Liu, S. (2019). *A novel calcium-chelating peptide purified from Auxis thazard protein hydrolysate and its binding properties with calcium*. *Journal of Functional Foods*, *60*, 103447. https://doi.org/10.1016/j.jff.2019.103447.

Dang, C. V., Shin, C. K., Bell, W. R., Nagaswami, C., & Weisel, J. W. (1989). *Fibrinogen sialic acid residues are low affinity calcium-binding sites that influence fibrin assembly*. *Journal of Biological Chemistry*, *264*(25), 15104–15108. https://doi.org/10.1016/S0021-9258(18)63817-7.

Farías, M. E., Martinez, M. J., & Pilosof, A. M. R. (2010). *Casein glycomacropeptide pH-dependent self-assembly and cold gelation*. *International Dairy Journal*, *20*, 79–88. http://www.sciencedirect.com/science/article/B6T7C-4X9TTSY-1/2/257c1f51231da5b85b32f0abd8b33dd2.

Fernando, S. F., & Woonton, B. W. (2010). *Quantitation of N-acetylneuraminic (sialic) acid in bovine glycomacropeptide (GMP)*. *Journal of Food Composition and Analysis*, *23*(4), 359–366. http://www.sciencedirect.com/science/article/B6WJH-4YH4PY0-1/2/10b7c7e6d5c36ae36499203ad47b6580.

Follows, D., Holt, C., Thomas, R. K., Tiberg, F., Fragneto, G., & Nylander, T. (2011). *Co-adsorption of β-casein and calcium phosphate nanoclusters (CPN) at hydrophilic and hydrophobic solid–solution interfaces studied by neutron reflectometry*. *Food Hydrocolloids*, *25*(4), 724–733. https://doi.org/10.1016/j.foodhyd.2010.09.001.

Gülseren, İ., Fang, Y., & Corredig, M. (2012). *Zinc incorporation capacity of whey protein nanoparticles prepared with desolvation with ethanol*. *Food Chemistry*, *135*(2), 770–774. https://doi.org/10.1016/j.foodchem.2012.04.146.

Guo, Q., Su, J., Xie, W., Tu, X., Yuan, F., Mao, L., et al. (2020). *Curcumin-loaded pea protein isolate-high methoxyl pectin complexes induced by calcium ions: Characterization, stability and in vitro digestibility*. *Food Hydrocolloids*, *98*, 105284. https://doi.org/10.1016/j.foodhyd.2019.105284.

Jaques, L. W., Brown, E. B., Barrett, J. M., Brey, W. S., & Weltner, W. (1977). *Sialic acid: A calcium-binding carbohydrate*. *Journal of Biological Chemistry*, *252*(No 13), 4533–4538.

Jiang, Y., Liu, X.-C., de Zawadzki, A., & Skibsted, L. H. (2021). *Binding of calcium to l-serine and o-phospho-l-serine as affected by temperature, pH and ionic strength under milk processing conditions*. *International Dairy Journal*, *112*, 104875. https://doi.org/10.1016/j.idairyj.2020.104875.

Jung, W.-K., Karawita, R., Heo, S.-J., Lee, B.-J., Kim, S.-K., & Jeon, Y.-J. (2006). *Recovery of a novel Ca-binding peptide from Alaska Pollack (Theragra chalcogramma) backbone by pepsinolytic hydrolysis*. *Process Biochemistry*, *41*(9), 2097–2100. https://doi.org/10.1016/j.procbio.2006.05.008.

Khajehpour, M., Dashnau, J. L., & Vanderkooi, J. M. (2006). *Infrared spectroscopy used to evaluate glycosylation of proteins*. *Analytical Biochemistry*, *348*(1), 40–48. https://doi.org/10.1016/j.ab.2005.10.009.

Kong, X., Bao, S., Song, W., Hua, Y., Zhang, C., Chen, Y., et al. (2021). *Contributions of ethanol fractionation on the properties of vegetable protein hydrolysates and differences in the characteristics of metal (Ca, Zn, Fe)-chelating peptides*. *LWT- Food Science and Technology*, *146*, 111482. https://doi.org/10.1016/j.lwt.2021.111482.

Korhonen, H., & Pihlanto, A. (2006). *Bioactive peptides: Production and functionality*. *International Dairy Journal*, *16*(9), 945–960. https://doi.org/10.1016/j.idairyj.2005.10.012.

Kreuß, M., Strixner, T., & Kulozik, U. (2009). *The effect of glycosylation on the interfacial properties of bovine caseinomacropeptide*. *Food Hydrocolloids*, *23*(7), 1818–1826. https://doi.org/10.1016/j.foodhyd.2009.01.011.

Lewis, S. P., Lewis, A. T., & Lewis, P. D. (2013). *Prediction of glycoprotein secondary structure using ATR-FTIR*. *Vibrational Spectroscopy*, *69*, 21–29. https://doi.org/10.1016/j.vibspec.2013.09.001.

Loria, K. G., Aragón, J. C., Torregiani, S. M., Pilosof, A. M. R., & Farías, M. E. (2018). *Flow properties of caseinomacropeptide aqueous solutions: Effect of particle size distribution, concentration, pH and temperature*. *LWT- Food Science and Technology*, *93*, 243–248. https://doi.org/10.1016/j.lwt.2018.03.050.

Loria, K. G., Pilosof, A. M. R., & Farías, M. E. (2018). *Influence of calcium and sodium chloride on caseinomacropeptide self-assembly and flow behaviour at neutral pH*. *LWT-Food Science and Technology*, *98*, 598–605. https://doi.org/10.1016/j.lwt.2018.09.029.

Luo, J., Yao, X., Soladoye, O. P., Zhang, Y., & Fu, Y. (2022). *Phosphorylation modification of collagen peptides from fish bone enhances their calcium-chelating and antioxidant activity*. *LWT- Food Science and Technology*, *155*, 112978. https://doi.org/10.1016/j.lwt.2021.112978.

Martinez, M. J., Carrera Sánchez, C., Patino, J. M. R., & Pilosof, A. M. R. (2009). *Bulk and interfacial behaviour of caseinoglycomacropeptide (GMP)*. *Colloids and Surfaces B: Biointerfaces*, *71*, 230–237.

Martinez, M. J., Carrera Sánchez, C., Rodríguez Patino, J. M., & Pilosof, A. M. R. (2012). *Interactions between β-lactoglobulin and casein glycomacropeptide on foaming*. *Colloids and Surfaces B: Biointerfaces*, *89*, 234–241. http://www.sciencedirect.com/science/article/pii/S0927776511005455.

Mekmene, O., & Gaucheron, F. (2011). *Determination of calcium-binding constants of caseins, phosphoserine, citrate and pyrophosphate: A modelling approach using free calcium measurement*. *Food Chemistry*, *127*(2), 676–682. https://doi.org/10.1016/j.foodchem.2010.12.121.

Ney, D. M., Hull, A. K., van Calcar, S. C., Liu, X., & Etzel, M. R. (2008). *Dietary Glycomacropeptide supports growth and reduces the concentrations of phenylalanine in plasma and brain in a murine model of phenylketonuria*. *Journal of Nutrition*, *138*(2), 316–322. http://jn.nutrition.org/cgi/content/abstract/138/2/316.

Peng, Z., Hou, H., Zhang, K., & Li, B. (2017). *Effect of calcium-binding peptide from Pacific cod (Gadus macrocephalus) bone on calcium bioavailability in rats*. *Food Chemistry*, *221*, 373–378. https://doi.org/10.1016/j.foodchem.2016.10.078.

Recio, R. T., Guerra, N. P., Torrado, A., & Skibsted, L. H. (2019). *Interaction between calcium and casein hydrolysates: Stoichiometry, binding constant, binding sites and thermal stability of casein phosphopeptide complexes*. *International Dairy Journal*, *88*, 25–33. https://doi.org/10.1016/j.idairyj.2018.08.009.

Roig, M. J., Alegría, A., Barberá, R., Farré, R., & Lagarda, M. J. (1999). *Calcium bioavailability in human milk, cow milk and infant formulas-comparison between dialysis and solubility methods*. *Food Chemistry*, *65*, 353–357.

Sunds, A. V., Poulsen, N. A., & Larsen, L. B. (2019). *Short communication: Application of proteomics for characterization of caseinomacropeptide isoforms before and after desialidation*. *Journal of Dairy Science*, *102*(10), 8696–8703. https://doi.org/10.3168/jds.2019-16617.

Thöma-Worringer, C., Sørensen, J., & López-Fandiño, R. (2006). *Health effects and technological features of caseinomacropeptide*. *International Dairy Journal*, *16*, 1324–1333.

Valente, A. J. M., Ribeiro, A. C. F., Rita, M. B. B. J., Carvalho, R. A., Esteso, M. A., & Lobo, V. M. M. (2011). *Transport properties of aqueous solutions of calcium lactate in the absence and presence of β-cyclodextrin*. *Journal of Molecular Liquids*, *161*(3), 125–131. https://doi.org/10.1016/j.molliq.2011.05.004.

Vavrusova, M., & Skibsted, L. H. (2014). *Calcium nutrition. Bioavailability and fortification*. *Lebensmittel-Wissenschaft und -Technologie- Food Science and Technology*, *59*(2), 1198–1204. https://doi.org/10.1016/j.lwt.2014.04.034.

Wang, X., Gao, A., Chen, Y., Zhang, X., Li, S., & Chen, Y. (2017). *Preparation of cucumber seed peptide-calcium chelate by liquid state fermentation and its characterization*. *Food Chemistry*, *229*, 487–494. https://doi.org/10.1016/j.foodchem.2017.02.121.

Wu, W., He, L., Liang, Y., Yue, L., Peng, W., Jin, G., et al. (2019). *Preparation process optimization of pig bone collagen peptide-calcium chelate using response surface methodology and its structural characterization and stability analysis*. *Food Chemistry*, *284*, 80–89. https://doi.org/10.1016/j.foodchem.2019.01.103.

Xu, Z., Wu, C., Sun-Waterhouse, D., Zhao, T., Waterhouse, G. I. N., Zhao, M., et al. (2021). *Identification of post-digestion angiotensin-I converting enzyme (ACE) inhibitory peptides from soybean protein Isolate: Their production conditions and in silico molecular docking with ACE*. *Food Chemistry*, *345*, 128855. https://doi.org/10.1016/j.foodchem.2020.128855.

Zhang, X., Geng, F., Huang, X., & Ma, M. (2016). *Calcium binding characteristics and structural changes of phosvitin*. *Journal of Inorganic Biochemistry*, *159*, 76–81. https://doi.org/10.1016/j.jinorgbio.2016.02.001.

Zhang, X., Jia, Q., Li, M., Liu, H., Wang, Q., Wu, Y., et al. (2021). *Isolation of a novel calcium-binding peptide from phosvitin hydrolysates and the study of its calcium chelation mechanism*. *Food Research International*, *141*, 110169. https://doi.org/10.1016/j.foodres.2021.110169.

Zhao, L., Huang, S., Cai, X., Hong, J., & Wang, S. (2014). *A specific peptide with calcium chelating capacity isolated from whey protein hydrolysate*. *Journal of Functional Foods*, *10*, 46–53. https://doi.org/10.1016/j.jff.2014.05.013.

Zhao, Z., Vavrusova, M., & Skibsted, L. H. (2018). *Antioxidant activity and calcium binding of isomeric hydroxybenzoates*. *Journal of Food and Drug Analysis*, *26*(2), 591–598. https://doi.org/10.1016/j.jfda.2017.07.001.

Zong, H., Peng, L., Zhang, S., Lin, Y., & Feng, F. (2012). *Effects of molecular structure on the calcium-binding properties of phosphopeptides*. *European Food Research and Technology*, *235*(5), 811–816. https://doi.org/10.1007/s00217-012-1809-5.